A Novel Sine Duty-Cycle Modulation Control Scheme for Photovoltaic Single-Phase Power Inverters

ARNAUD OBONO BIYOBO
Research Laboratory of Computer Science Engineering and Automation
ENSET, University of Douala
Po. Box 1872, Douala,
CAMEROON
obonobiyo@yahoo.fr

LEANDRE NNEME NNEME
Research Laboratory of Computer Science Engineering and Automation
ENSET, University of Douala
Po. Box 1872, Douala,
CAMEROON
leandren@gmail.com

JEAN MBIHI
mbihidr@yahoo.fr, http://www.cyberquec.ca/mbihi/
Research Laboratory of Computer Science Engineering and Automation
ENSET, University of Douala
Po. Box 1872, Douala,
CAMEROON

Abstract: - In this paper, a novel SDCM (sine duty-cycle modulation) scheme for photovoltaic (PV) single-phase power inverter is presented. Unlike popular SPWM (sine pulse width modulation) strategies, the SDCM control scheme consists of a minimum number or building components, while offering a robust feedback control topology. The main DC power to be converted, is delivered by an upstream PV panel. Then, a SDCM circuit with appropriate basic modulation frequency, is used as a switching driver for power MOSFETs of a single phase H-bridge inverter. The merits of the proposed SDCM control scheme, are proven using analytical developments, followed by relevant virtual simulations conducted on a prototyping power inverter within Multisim software framework. Moreover, the virtual simulation results obtained are presented, in order to show the high quality of the proposed class of SDCM control schemes for PV Single-phase power inverters.

Key-Words: - Sine duty-cycle modulation, control scheme, open-loop control, photovoltaic, single-phase, power inverters, LC filter, virtual simulation.

1 Introduction

A power inverter is a controlled interfacing systems, between a main DC energy source and an AC load to be supplied. Although power inverters are widely encountered in industrial electronics for a wide variety of technical applications, they are increasingly used nowadays in solar power systems [1-3]. A number of research works have been published so far on single-phase PV (photovoltaic) inverters [4-7]. However, in most of these pioneering works, the great emphasis is on the improvement or extension of existing SPWM (sine pulse width modulation) control strategy for PV-based energy systems. Moreover, according to a few available recent scientific papers, many weaknesses are hidden behind the basic PWM (pulse width modulation) principle, e.g., complexity of triangle modulation clock, open-loop control topology, constant modulation frequency and more.

The originality of this research paper is to study a novel high frequency switching modulation topology for single-phase power inverters for single-phase AC loads. It is founded on a simple DCM (duty-cycle modulation) strategy, initiated earlier since 2005 [8] for industrial instrumentation purpose. Over years, it has been increasingly used further as a versatile modulation technique, for solving a wide variety of instrumentation problems, including ADC (analog-to-digital conversion)[9]-[10], DAC (digital-to-analog conversion) [11-13], and analog signal transmission [14-16]. However, according to our best knowledge, the first recent applications of DCM control schemes in power electronics is restricted to the class of DC-DC power converters, e.g., Buck converters [17], Boost converters [18] and new digital modulation drivers [19].

Therefore, the novelty of this paper is to show from analytical developments and virtual simulation basis, that unlike popular SPWM (sine pulse width modulation) strategies with hidden relevant weaknesses, the proposed novel SDCM (sine duty-cycle modulating) control scheme, offers minimum hardware simplicity, lower implementation costs, attractive modulation properties and quality for PV-based single-phase inverters.

In section 2 of this paper, the SDCM principle is outlined. Then, the SDCM control scheme for PV-based single-phase inverters is detailed in section 3. Furthermore, in section 3, virtual simulations is conducted on a prototyping power inverter system and the relevant results obtained and related findings are presented, followed by the conclusion of the paper in section 4.

2 Principle of SDCM Strategy

The SDCM strategy recalled in this section is a signal processing technique, allowing to transform a sine wave input u(t) = a sin(2π f_s t + θ) into a switching modulated wave $u_m(x(t)) \equiv u_m(t)$ with time varying pulse width $T_{on}(u(t)) \equiv T_{on}(t)$ and period $T_m(u(t)) \equiv T_m(t)$. In that case, the modulating input can be recovered from the DCM function $R_m(x(t)) \equiv R(t)$ where $R_m(t) = T_{on}(t)/T_m(t)$. Although the SDCM principle seems apparently intricate, it is fortunately surprising to discover as shown in Fig. 1 that, compared to a basic PWM circuit (Fig. 1(a)), a DCM circuit (Fig. 1(a) however relies on minimum building components. Indeed, it consists of a single integrated operational amplifier, associated with four passive components with design parameters R1, R2, R3 and C1 respectively.

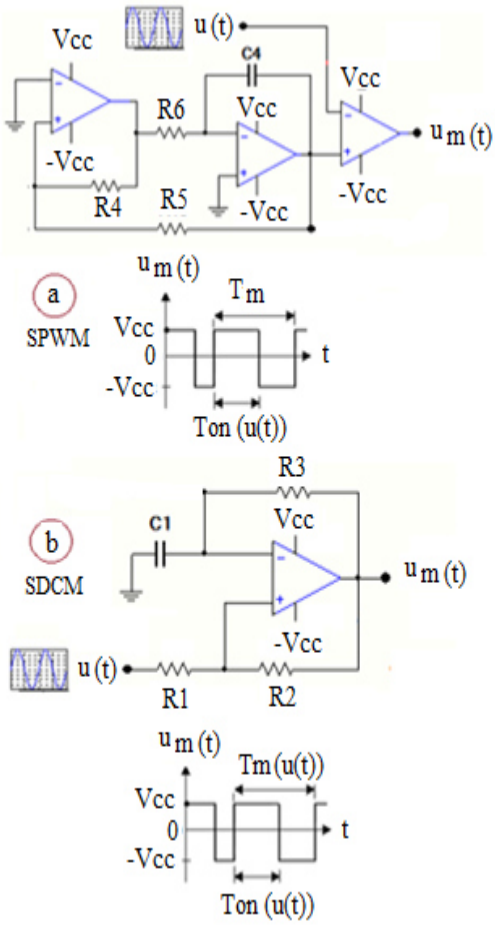

Fig. 1 SPWM (a) and SDCM (b) circuits

From Fig. 1(b), it is important to recall that the Fourier's series of the time varying periodic $T_m(u(t)) \equiv T_m(t)$ of the SDCM wave, could be written as follows ([11-15]):

$$u_m(u(t)) \equiv u_m(t) = C_0(u(t)) + \sum_{n=1}^{\infty}\left(C_n(u(t))\cos\left(2\,\pi\,n\frac{t}{T_m(u(t))}\right)\right) \quad (1)$$

where,

$$\begin{cases} C_0(u(t)) = \left(2\,R_m(u(t)) - 1\right) Vcc \\ C_n(u(t)) = \left(\dfrac{4\,Vcc}{\pi}\right)\dfrac{\sin\left(n\pi\,R_m(u(t))\right)}{n}, \quad n \geq 1 \end{cases} \quad (2)$$

$$R_m(u(t)) = \frac{T_{on}(u(t))}{T_m(u(t))} = \frac{\ln\left(\dfrac{\alpha_2 u(t) - (1+\alpha_1)\,Vcc}{\alpha_2 u(t) + (\alpha_1 - 1)\,Vcc}\right)}{\ln\left(\dfrac{(\alpha_2 u(t))^2 - ((1+\alpha_1)\,Vcc)^2}{(\alpha_2 u(t))^2 - ((\alpha_1 - 1)\,Vcc)^2}\right)} \quad (3)$$

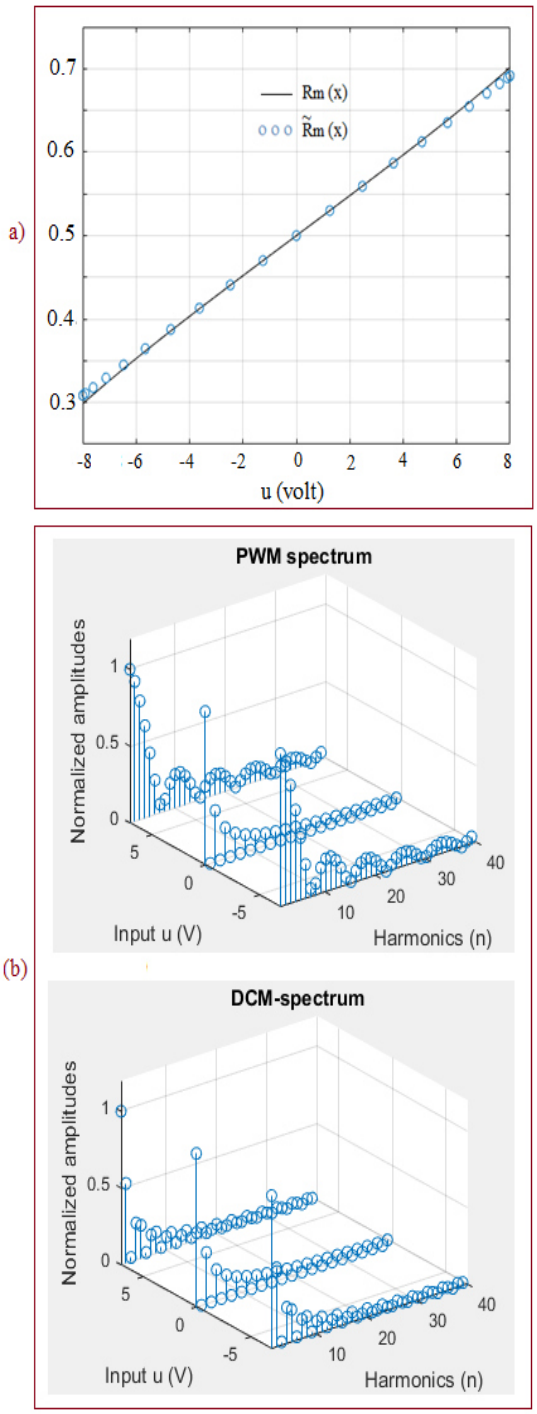

Fig. 2 Spectra of PWM and DCM waves for the same basic modulation frequency

It is important to outline the fact that for a SPWM strategy, the modulation period T_m in (1) is a pure constant parameter, while $R_m(u(t))$ in (2) is a linear function of u(t) since $T_{on}(u(t))$ and $T_{off}(u(t)) = T_m - T_{on}(u(t))$ are linear over the involved modulating space. Moreover, although (3) is apparently a dreadful nonlinear function, it has been shown that it is rigorously linear in a wide vicinity of the rating point (R_m=0, u=1/2). Therefore, the linear expression obtained from the first order Taylor series of (3) is given by,

$$\tilde{R}_m(x(u(t) = p_m u(t) + \frac{1}{2}, \quad \text{where}$$

$$p_m = \frac{\frac{\alpha_1}{Vcc\ (1+\alpha_1)}}{\log\left(\frac{1+\alpha_1}{1-\alpha_1}\right)} \qquad (4)$$

Moreover, the basic modulation period for u (t) = 0 is given by :

$$T_m(0) = 2\,R_3\,C_1\,\log\left(\frac{1+\alpha_1}{1-\alpha_1}\right) \text{ where } \alpha_1 = \frac{R_1}{R_1+R_2} \qquad (5)$$

As an illustrative example, given the following set of data {Vcc = 12 V, R1= 10k, R2= 8.2k, R = 10k, C = 2 nF }, the resulting graphs obtained for { $R_m(u(t))$, $\tilde{R}_m(u(t))$, PWM and DCM spectra}, and presented in Fig. 2. Fig. 2(1) shows that the linear approximation $\tilde{R}_m((u(t))$ is exactly closed to $R_m(u(t))$ in a wide range estimated to [-7 volts , 7 volts], with p_m = 0.0239 in (4) and {α1 = 0.5495, $T_m(0)$ = 1/20.24 kHz} in (1). In addition, as shown in Fig. 2(b) where the graphs of normalized PWM and DCM spectra are presented, it is clear that the PWM strategy with constant frequency $f_{pwm}(0) = 1/T_m(0)$), offers a greedy frequency spectrum compared to that of the DCM strategy. Moreover, another relevant finding emerging from Fig. 2(b) is that, the amplitude of DCM harmonics with rank multiple of 3 are null. That fact might be a merit for reducing stresses on power MOSFETs of the H-bridge inverter, while improving the quality of the AC load voltage downstream the power LC filter.

As a straightforward implication, the DCM wave $u_m(u(t))$ defined by (1)-(2), indicates that a modulating sine input given by u(t) = a sin(2π f_s t + θ) could be recovered from the DCM modulated wave $u_m(u(t))$ with an eroded harmonic spectrum, using an appropriate linear low-pass filter with gain given as follows :

$$k_m = \frac{1}{2p_m Vcc} = \frac{(1+\alpha_1)}{2\alpha_1} l\,\log\left(\frac{1+\alpha_1}{1-\alpha_1}\right) \qquad (6)$$

The palette of Equations (1)-(6) stands for the analytical demonstration of the SDCM principle used in this paper, as a novel building strategy for single-phase PV power inverters with pure sine output voltage.

3 SDCM Control Scheme for Single Phase Power Inverter

The schematic diagram of the proposed SDCM control scheme for PV single-phase power inverters is presented in Fig. 3.

The power electronics topology is not new and consists of a solar medium, a PV panel with E = 2 x 12 (volts), a single phase H-bridge MOSFET inverter, a downstream low-pass filter, and an AC

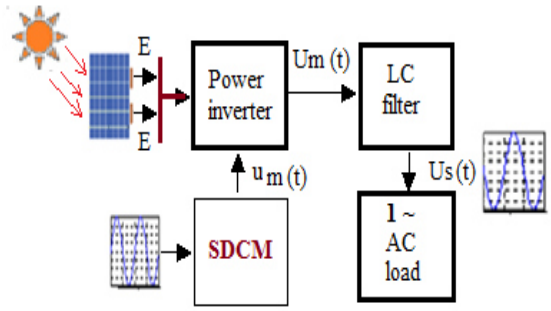

Fig. 3 SDCM scheme for single-phase PV power inverters

load to be supplied. Moreover, the four gates of power MOSFET switches are controlled from a sine modulating voltage u(t) = a sin(2π f_s t + θ), via a novel SDCM circuit described in the previous section.

Viewed from the SDCM output signal $u_m(x(t))$, the H-bridge MOSFET inverter exactly behaves under the sun lighting medium as a power amplifier with ideal static gain E/Vcc, whiles the resulting power modulated wave $U_m(x(t))$ has the same waveform and periodicity parameters (pulse width $T_{on}(x(t))$, period $T_m(x(t))$ than $u_m(x(t))$. In this case, the model of the switching power voltage delivered by the H-bridge MOSFET inverter, computed from (1)-(3) given that Rm(Us(t)) is dictated by Rm(x(t)), i.e., Rm(Us(t)) = Rm(x(t)), is given as follows :

$$U_m(u(t)) \equiv U_m(t) = A_0(u(t)) + \sum_{n=1}^{\infty}\left(A_n(u(t))\cos\left(2\,\pi\,n\frac{t}{T_m(u(t))}\right)\right) \quad (7)$$

where,

$$\begin{cases} A_0(u(t)) = \left(2\,R_m(u(t)) - 1\right)E \\ A_n(u(t)) = \left(\dfrac{4\,E}{\pi}\right)\dfrac{\sin\left(n\pi\,R_m(u(t))\right)}{n}, \; n \geq 1 \end{cases} \quad (8)$$

with,

$$\tilde{R}_m(x(u(t) = p_m u(t) + \frac{1}{2} \quad (9)$$

where,

$$p_m = \frac{\dfrac{\alpha_1}{Vcc\ (1+\alpha_1)}}{\log\left(\dfrac{1+\alpha_1}{1-\alpha_1}\right)} \quad (10)$$

Because of the similarity of (1)-(2) and (7)-(8), and according to the SDCM principle, the power image Us(t) of the modulating input u(t) encapsulated in $U_m(x(t))$, can be recovered upstream the AC load to be supplied, using a suitable low-pass LC filter with static gain depending on a given supplying AC voltage required by the load.

4 Case Study of an SDCM Control Scheme for PV Power Converter

The virtual model of the prototyping SDCM control scheme for PV single-phase power inverters in presented in Fig. 3. The numbers of building parts are 1 (Main DC power supply from PV panel), 2 (H-bridge IRF840 MOSFET inverter), 3 (low-pass LC filter), 4 (load with terminal power resistance Ro = 250Ω), 5 (Vcc voltage source), 6 (low frequency signal source for u(t) = 4 sin(2π 50 t + θ) volts, 7 (SDCM circuit), 8 (logic conformer), 9 (Virtual oscilloscope for the measurements of u(t) and $u_m(u(t))$ waves) and 10 (virtual oscilloscope for the measurement of u(t) and the related response Us(t) at the load terminals.

Recall that the SDCM circuit used in Fig. 4 is the same as that presented earlier in the illustrative example (see Fig. 2)), where $f_m(0) = 1/T_m(0)$ = 20.24 kHz. Recall also that Ua-Ub in Fig. 4 is equal to the power switching input voltage Um(u(t)) of the low-pass LC filter. Moreover, the transfer function of that LC filter is given as follows:

$$F(s) = \frac{Us(s)}{Um(s)} = \frac{1}{L\,C\,s^2 + R\,C\,s + 1} \quad (11)$$

The bode diagram of the LC filter obtained under Matlab framework using R = 200 mH, L = 150 mH, C = 66uF is presented in Fig. 5. It is important to observe that the modulating frequency of 50 Hz required by the terminal AC load lies within the pass-band of the low-pass filter, and the basic modulation frequency $f_m(0)$ = 20.24 kHz is so far from 50 Hz that it should be cut off completely. As an implication, the predicted load voltage Us(t) will be absolutely a pure sine wave.

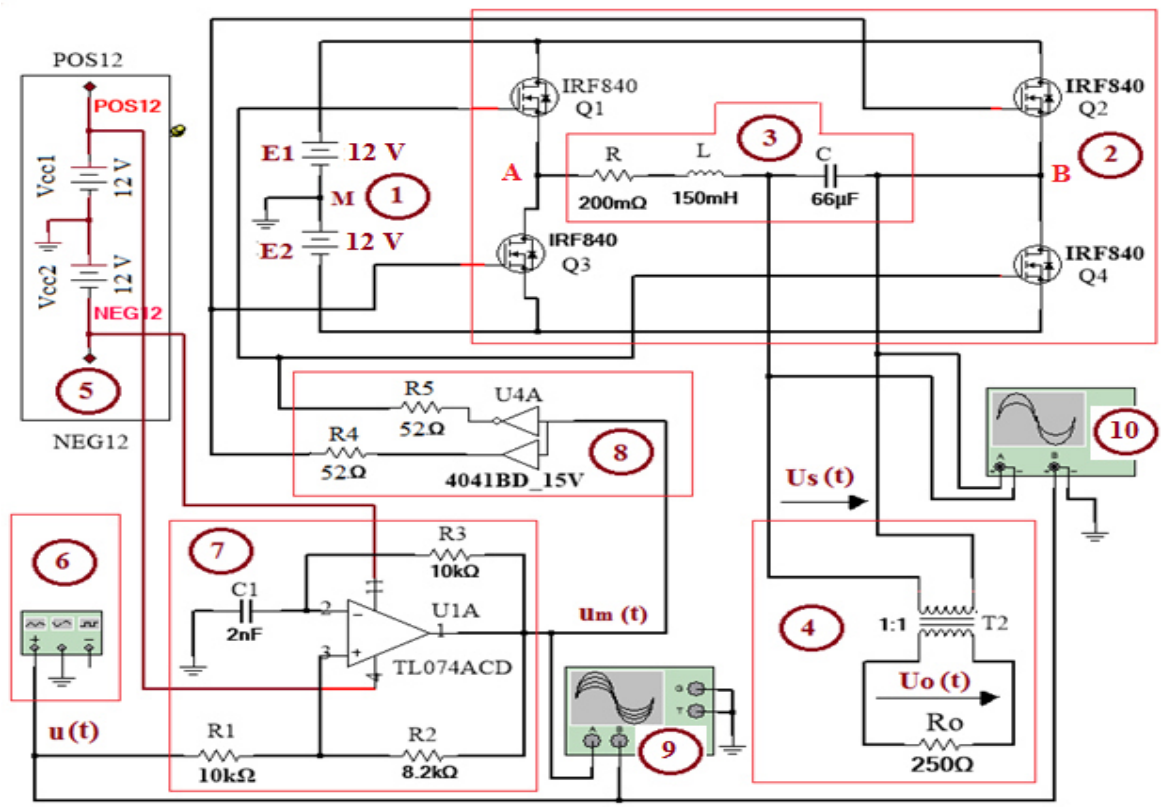

Fig. 4 Virtual model of prototyping SDCM control Scheme for PV single-phase power inverter

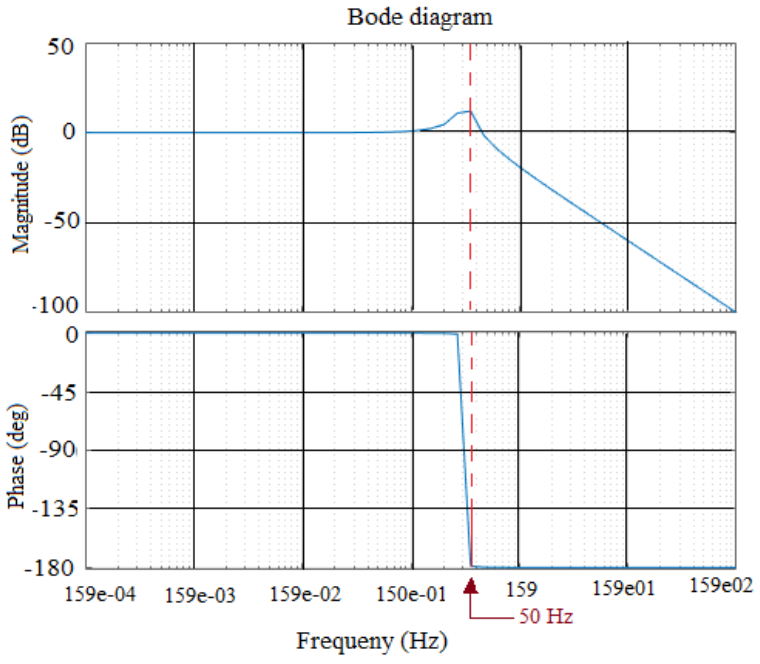

Fig. 5 Bode diagrams of the low-pass LC filter

The modulating and modulated signals of the SDCM circuit obtained when simulating the prototyping virtual SDCM power inverter system, are presented in Fig. 6, where the amplitude of $u_m(t)$ is a = 4 volts and the switching threshold levels of xm(t) are ±Vcc = ±12 V.

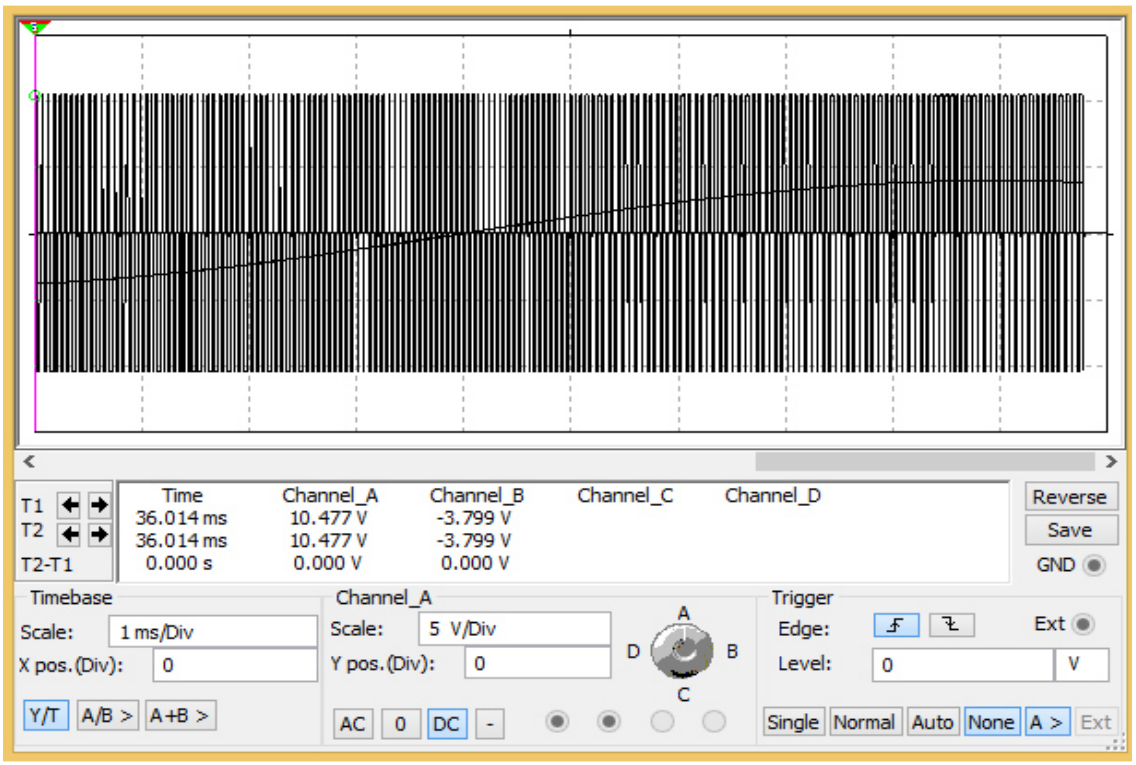

Fig. 6 Shape of signals u(t) and um(x(t)) of the SDCM driver

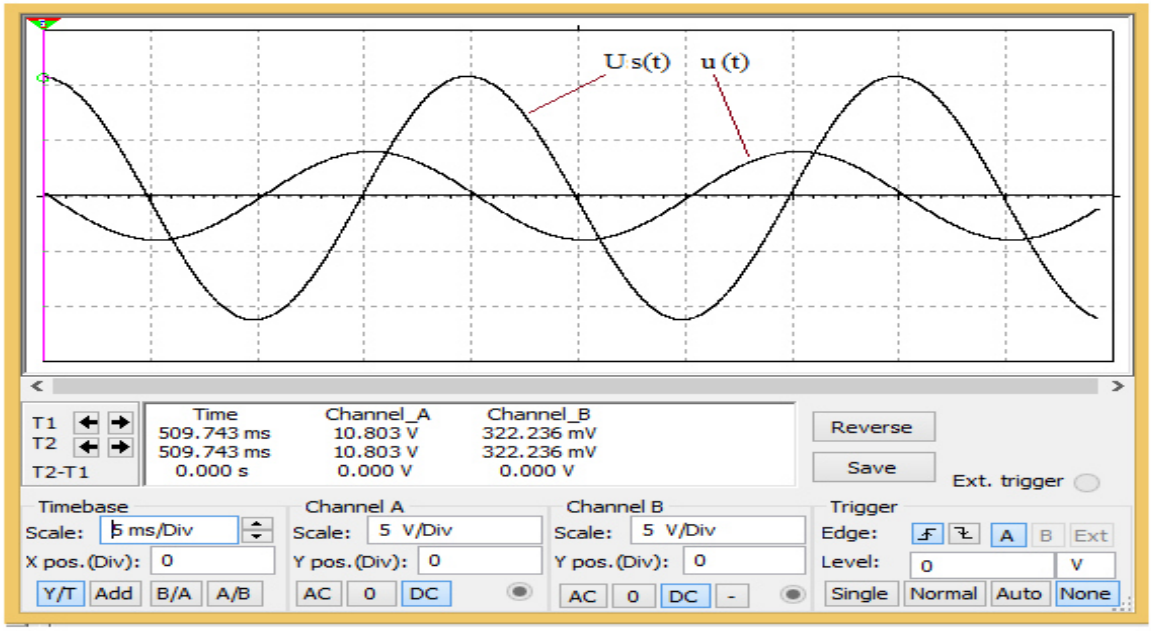

Fig. 7 Shapes of the modulation signal u(t) and the power voltage Us(t) for (Ro = 250 Ω)

In addition, Fig. 6 shows the shapes of the modulating signal u(t) and the power voltage $u_m(t)$, whereas in Fig. 7, u(t) and the predicted voltage Us(t) delivered to the load is a pure AC sine voltage, with basic frequency fs = 50 Hz, and stable amplitude a = 11.5 volts which can be shifted freely if needed, using an appropriate power transformer (see Fig. 4).

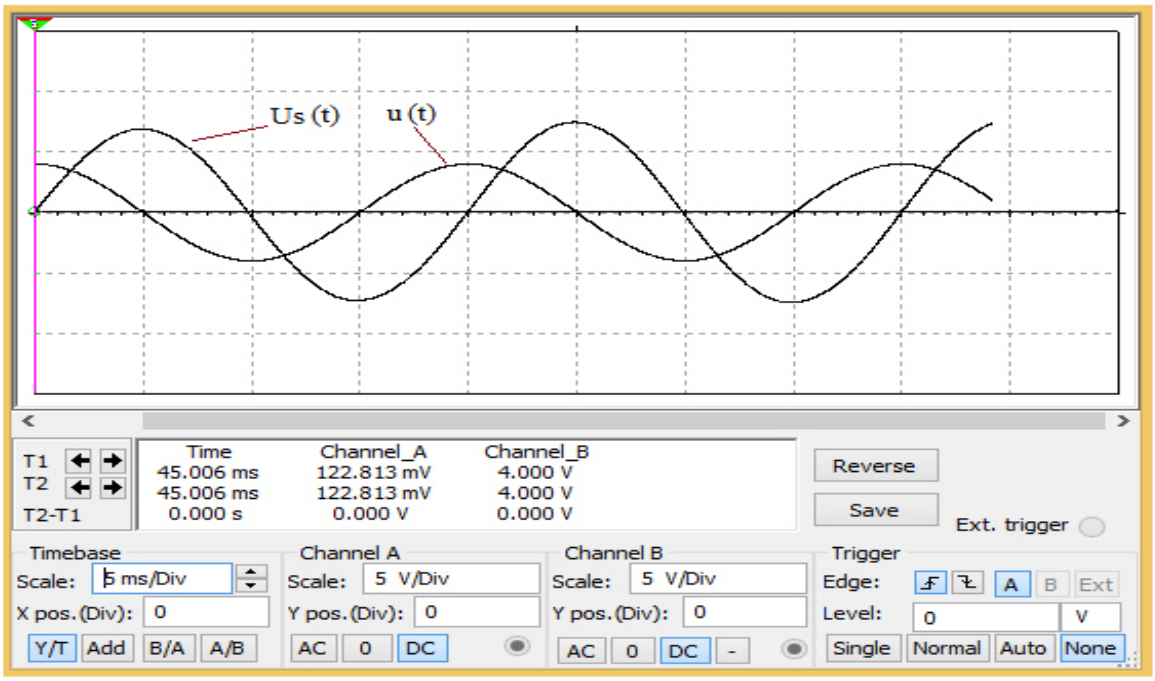

Fig. 8 Shapes of the modulation signal u(t) and the power voltage Us(t) for (Ro = 150 Ω)

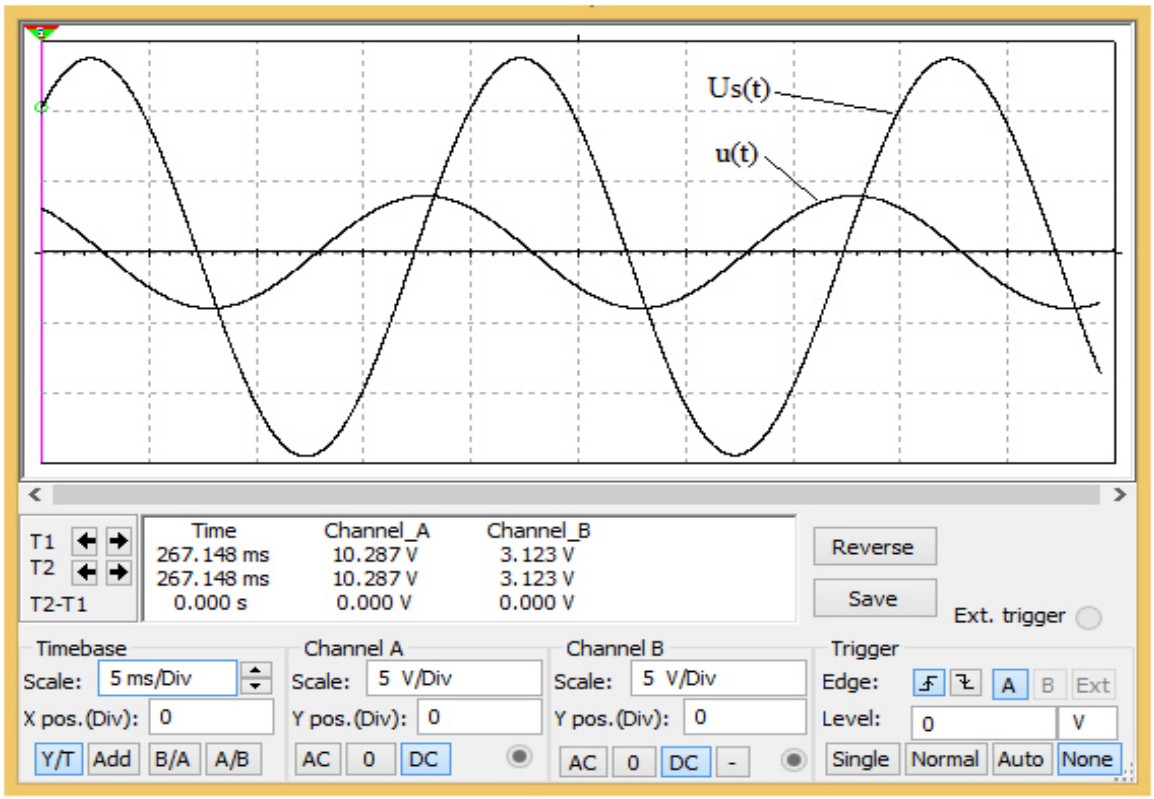

Fig. 9 Shapes of the modulation signal u(t) and the power voltage Us(t) for (Ro = 350 Ω)

Before to conclude this paper, it is also important to point out the fact that the well tested novel SDCM control scheme presented in this research work, is an open loop control scheme. As a consequence, disturbances due to load changes might lead to significant variations of the supplied voltage Us(t) as shown in Fig. 8 for higher power demand, e.g., Ro = 150 Ω. Moreover, as presented in Fig. 9, a lower power demand, e.g;, Ro = 350 Ω, might also leads to an unpredictable increase in the load voltage Us(t).

In all cases, the undesired effects of unpredictable disturbances, even poor static and dynamic performances, are the common weaknesses of all open-loop dynamic control systems. Such intricate phenomena can be satisfactory cancelled using standard feedback control strategies available in automatic feedback control practise.

5 Conclusion

The novelty of the SDCM control principle presented in this paper for single phase PV power inverters has been proven, using analytical developments as well as computer-aided simulations of a well tested virtual system. In future research works, it would be interesting to transform the virtual reality study into realistic implementation. In would be appreciable also to overcome the weaknesses of open-loop controls by robust feedback control strategies.

ACKNOWLEDGEMENTS

The authors of this research works wishes to acknowledge the great relevant effects of the *scientific research grant* offered by the *Ministry of Higher Education* of Cameroon. It has facilitated the access to support and technical research resources needed for most editing activities involved in this research work

REFERENCES

[1] B. M. Sharma, New Trends in Solar Energy Modeling and Developing a Relation for Performance of Solar Radiation, *European Jurnal of Advances in Engineering and Technology*, 2017, 4(9), 649-656.

[2] H. Koran, T. LaBella and J-S. Lai, High Efficiency Photovoltaic Source Simulator with Fast Response Time for Solar Power Conditioning Systems Evaluation, *IEEE Transactions on Power Electronics,* **2014,** 29 (3), 1285-1296.

[3] R Wai and W Wang, Grid-Connected Photovoltaic Generation System, *IEEE Transaction on Circuits and Sys-tems*, 2008, 55 (3), 953–964.

[4] A.A Hassan, F. Famy, A. E.A Nafeh, M. A. and El-Sayyed, Modelling and Simulation of a single phase grid connected photovoltaic system, Wseas Transactions on Systems and Control, January 2010, 1(5), 16-25.

[5] M. Dave and S. R. Vyas, Simulation and modelling of single phase DC-AC converter for solar inverter, *International Research Journal of Engineering and Technology*, December 2015, 02(9), pp. 2225-2230.

[6] S. M. Cherati, N. A. Azili, M. Ayob and A. Mortezaei, Design of a current mode PI controller for a single phase PWM Inverter, *IEEE Applied Power Electronics Colloquim*, 2011, pp. 180-183.

[7] K. G. Gosmni and G. GhoshZhan,Closed loop PI design of single-phase motor using SPWM, *International Journal of Advances Research in Computer Science and Software Engineering*, 2017, 7(6), pp. 123-128.

[8] Mbihi, B. Ndjali and M. Mbouenda, Modelling and Simulation of a Class of Duty-Cycle modulators for Industrial Instrumentation, *Iranian Journal of Electrical and Computer Engineering*, 2005, 4(2), pp. 121-128.

[9] Mbihi, B. Ndjali and M. Mbouenda, A novel Analog-To-Digital Conversion Technique Using Duty-Cycle Modulation, *International Journal of Electronics and Computer Science Engineering*, 2012, 1(3), pp. 818-825.

[10] J. Mbihi and L. Nneme Nneme, A Multi-Channel Analog-To-Digital Conversion Technique Using Parallel Duty-Cycle Modulation, *International Journal of Electronics and Computer Science Engineering*, 2012, 1(3), pp. 826–833.

[11] Moffo Lonla B., Mbihi J., Nneme Nneme L., Kom M., A Novel Digital– to–Analog Conversion Technique using Duty-Cycle Modulation, *International Journal of Circuits, Systems and Signal processing,* 2013.

[12] B. Moffo Lonla. And J. Mbihi, A Novel Digital Duty–Cycle Modulation Scheme for FPGA-Based Digital-to-Analog Conversion, *IEEE Transaction on circuits and system II*, 2015, 62(6), pp. 543–547.

[13] B. Moffo Lonla, J. Mbihi and L. Nneme Nneme, FPGA-Based Multichannel Digital Duty-cycle Modulation and application to simultaneous Generation of Analog Signals, STM *Journal of Electronic Design Technology (JoEDT)*, 2017, 8(1), pp. 23-35.

[14] L. Nneme Nneme, J. Mbihi, Modeling and Simulation of a New Duty– Cycle Modulation

Scheme for Signal Transmission System, *American Journal of Electrical and Electronic Engineering,* 2014, 2(3), pp. 82–87

[15] Moffo Lonla B., Jean Mbihi, Leandre Nneme Nneme. A Low Cost and High Quality Duty–Cycle Modulation Scheme and Applications. *International Journal of Electrical, Electronic Science and Engineering*, 2014, 8(3), pp. 82–88.

[16] Mbihi, Nneme, Kom, A Suboptimal Nonlinear Duty-cycle Modulation Scheme, © STM *Journal of electronic Design Technology*, 2016, 7(1), pp. 22-31.

[17] J. Mbihi and L. Nneme Nneme, "A Novel Control Scheme for Buck Power Converters using Duty–Cycle Modulation". *International Journal of Power Electronics*, 2013, 5(3/4), pp. 185–199.

[18] Y. P. Danwé Sounsoumou, H. Djalo, J. Mbihi, et J. Y. Effa, Modelisation Virtuelle d'un nouveau schema de réglage de Boost à commande rapprochée par modulation en rapport cyclique, *Journal Afrique Science*, 13(11), 2017, pp. 176-185.

[19] J. Mbihi, Dynamic modelling and virtual simulation of duty-cycle modulation control drivers, *International Journal of Electrical, Electronic Science and Engineering*, 2017, 11(4), pp. 472-477.